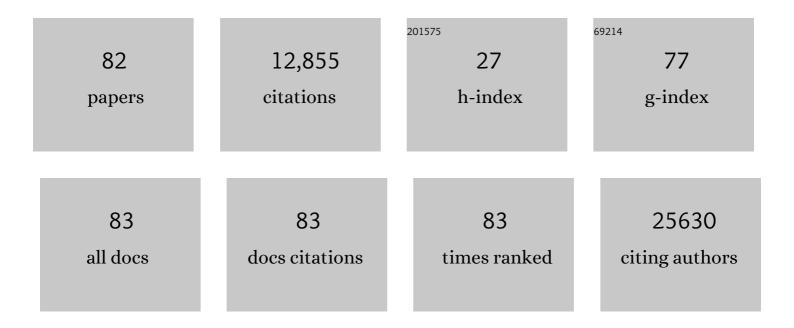
Liang Wang

List of Publications by Year in descending order

Source: https://exaly.com/author-pdf/8563061/publications.pdf Version: 2024-02-01



LIANC WANC

#	Article	IF	CITATIONS
1	Preliminary assessment of a portable Raman spectroscopy system for post-operative urinary stone analysis. World Journal of Urology, 2022, 40, 229-235.	1.2	4
2	Quality in MR reporting (include improvements in acquisition using AI). British Journal of Radiology, 2022, 95, 20210816.	1.0	2
3	A pH-Dependent rhodamine fluorophore with antiproliferative activity of bladder cancer inÂVitro/Vivo and apoptosis mechanism. European Journal of Medicinal Chemistry, 2022, 236, 114293.	2.6	4
4	Noninvasive Differentiation of Obstructive Azoospermia and Nonobstructive Azoospermia Using Multimodel Diffusion Weighted Imaging. Academic Radiology, 2021, 28, 1375-1382.	1.3	2
5	Refractory lower urinary tract symptoms in patients with lumbar disc hernia relieved by non-surgical treatment. World Journal of Urology, 2021, 39, 1597-1605.	1.2	0
6	Value of Intra-Perinodular Textural Transition Features from MRI in Distinguishing Between Benign and Malignant Testicular Lesions. Cancer Management and Research, 2021, Volume 13, 839-847.	0.9	4
7	Predictive role of T2WI and ADC-derived texture parameters in differentiating Gleason score 3 + 4 and 4 + 3 prostate cancer. Journal of X-Ray Science and Technology, 2021, 29, 307-315.	0.7	1
8	CircLIFR synergizes with MSH2 to attenuate chemoresistance via MutSα/ATM-p73 axis in bladder cancer. Molecular Cancer, 2021, 20, 70.	7.9	46
9	Melatonin inhibits lipid accumulation to repress prostate cancer progression by mediating the epigenetic modification of CES1. Clinical and Translational Medicine, 2021, 11, e449.	1.7	22
10	Long-term chest CT follow-up in COVID-19 Survivors: 102–361 days after onset. Annals of Translational Medicine, 2021, 9, 1231-1231.	0.7	16
11	Demographic, signs and symptoms, imaging characteristics of 2126 patients with COVID-19 pneumonia in the whole quarantine of Wuhan, China. Clinical Imaging, 2021, 77, 169-174.	0.8	2
12	<i>Circ0008399</i> Interaction with WTAP Promotes Assembly and Activity of the m6A Methyltransferase Complex and Promotes Cisplatin Resistance in Bladder Cancer. Cancer Research, 2021, 81, 6142-6156.	0.4	86
13	Preparing for future waves and pandemics: a global hospital survey on infection control measures and infection rates in COVID-19. Antimicrobial Resistance and Infection Control, 2021, 10, 170.	1.5	2
14	Epigenetic and Immune-Cell Infiltration Changes in the Tumor Microenvironment in Hepatocellular Carcinoma. Frontiers in Immunology, 2021, 12, 793343.	2.2	21
15	Prevalence and changes of BMI categories in China and related chronic diseases: Cross-sectional National Health Service Surveys (NHSSs) from 2013 to 2018. EClinicalMedicine, 2020, 26, 100521.	3.2	35
16	Combined multiple clinical characteristics for prediction of discordance in grade and stage in prostate cancer patients undergoing systematic biopsy and radical prostatectomy. Pathology Research and Practice, 2020, 216, 153235.	1.0	2
17	circNR3C1 Suppresses Bladder Cancer Progression through Acting as an Endogenous Blocker of BRD4/C-myc Complex. Molecular Therapy - Nucleic Acids, 2020, 22, 510-519.	2.3	19

18 Resolving Seemingly Conflicting Fact Statements Caused by Missing Terms. , 2020, , .

0

#	Article	IF	CITATIONS
19	Added Value of Biparametric MRI and TRUS-Guided Systematic Biopsies to Clinical Parameters in Predicting Adverse Pathology in Prostate Cancer. Cancer Management and Research, 2020, Volume 12, 7761-7770.	0.9	3
20	Predicting Prostate Cancer Upgrading of Biopsy Gleason Grade Group at Radical Prostatectomy Using Machine Learning-Assisted Decision-Support Models. Cancer Management and Research, 2020, Volume 12, 13099-13110.	0.9	10
21	Water-stable and finasteride-loaded polyvinyl alcohol nanofibrous particles with sustained drug release for improved prostatic artery embolization — In vitro and in vivo evaluation. Materials Science and Engineering C, 2020, 115, 111107.	3.8	9
22	Discrimination between benign and malignant testicular lesions using volumetric apparent diffusion coefficient histogram analysis. European Journal of Radiology, 2020, 126, 108939.	1.2	13
23	Genomic characterisation and epidemiology of 2019 novel coronavirus: implications for virus origins and receptor binding. Lancet, The, 2020, 395, 565-574.	6.3	9,430
24	Sight and switch off: Nerve density visualization for interventions targeting nerves in prostate cancer. Science Advances, 2020, 6, eaax6040.	4.7	28
25	What can European radiologists learn from the outbreak of COVID-19 in China? A discussion with a radiologist from Wuhan. European Radiology, 2020, 30, 3609-3611.	2.3	12
26	IMPDH1/YB-1 Positive Feedback Loop Assembles Cytoophidia and Represents a Therapeutic Target in Metastatic Tumors. Molecular Therapy, 2020, 28, 1299-1313.	3.7	20
27	Prediction of Pathological Upgrading at Radical Prostatectomy in Prostate Cancer Eligible for Active Surveillance: A Texture Features and Machine Learning-Based Analysis of Apparent Diffusion Coefficient Maps. Frontiers in Oncology, 2020, 10, 604266.	1.3	12
28	Assessment of the Severity of Coronavirus Disease: Quantitative Computed Tomography Parameters versus Semiquantitative Visual Score. Korean Journal of Radiology, 2020, 21, 998.	1.5	31
29	Validation of SE-EPI-based T2 mapping for characterization of prostate cancer: a new method compared with the traditional CPMG method. Abdominal Radiology, 2019, 44, 3432-3440.	1.0	2
30	Bi-exponential versus mono-exponential diffusion-weighted imaging for evaluating prostate cancer aggressiveness after radical prostatectomy: a whole-tumor histogram analysis. Acta Radiologica, 2019, 60, 1566-1575.	0.5	4
31	CircCDYL inhibits the expression of C-MYC to suppress cell growth and migration in bladder cancer. Artificial Cells, Nanomedicine and Biotechnology, 2019, 47, 1349-1356.	1.9	29
32	Digital subtract angiography and lipiodol deposits following embolization in cirrhotic nodules of LIRADS category ≥3. European Journal of Radiology Open, 2019, 6, 106-112.	0.7	1
33	Multi-parametric MRI-based radiomics signature for discriminating between clinically significant and insignificant prostate cancer: Cross-validation of a machine learning method. European Journal of Radiology, 2019, 115, 16-21.	1.2	95
34	T2-Weighted Image-Based Radiomics Signature for Discriminating Between Seminomas and Nonseminoma. Frontiers in Oncology, 2019, 9, 1330.	1.3	23
35	Physical activity and sedentary time in relation to semen quality in healthy men screened as potential sperm donors. Human Reproduction, 2019, 34, 2330-2339.	0.4	33
36	Trends in smoking prevalence and implication for chronic diseases in China: serial national cross-sectional surveys from 2003 to 2013. Lancet Respiratory Medicine,the, 2019, 7, 35-45.	5.2	225

#	Article	IF	CITATIONS
37	Abbreviated Biparametric Versus Standard Multiparametric MRI for Diagnosis of Prostate Cancer: A Systematic Review and Meta-Analysis. American Journal of Roentgenology, 2019, 212, 357-365.	1.0	82
38	Long noncoding RNA GAS5 promotes bladder cancer cells apoptosis through inhibiting EZH2 transcription. Cell Death and Disease, 2018, 9, 238.	2.7	92
39	Effects of Echo Time on IVIM Quantification of the Normal Prostate. Scientific Reports, 2018, 8, 2572.	1.6	13
40	Multi-model Analysis of Diffusion-weighted Imaging of Normal Testes at 3.0 T. Academic Radiology, 2018, 25, 445-452.	1.3	4
41	Characterization of testicular germ cell tumors: Whole-lesion histogram analysis of the apparent diffusion coefficient at 3T. European Journal of Radiology, 2018, 98, 25-31.	1.2	15
42	Diagnostic Performance and Interobserver Consistency of the Prostate Imaging Reporting and Data System Version 2. Chinese Medical Journal, 2018, 131, 1666-1673.	0.9	9
43	Abernethy Malformation Type II and Concurrent Nodular Hyperplasia in a Rare Female Case. Case Reports in Radiology, 2018, 2018, 1-4.	0.5	0
44	MRI feature analysis of uncommon prostatic malignant tumors. Asian Journal of Andrology, 2018, 20, 313.	0.8	4
45	Using the prostate imaging reporting and data system version 2 (PI-RIDS v2) to detect prostate cancer can prevent unnecessary biopsies and invasive treatment. Asian Journal of Andrology, 2018, 20, 459.	0.8	19
46	Bochdalek hernia presenting with initial local fat infiltration of the thoracic cavity in a leukemic child. Radiology Case Reports, 2017, 12, 200-203.	0.2	1
47	Benign prostatic hyperplasia after prostatic arterial embolization in a canine model: A 3T multiparametric MRI and wholeâ€mount stepâ€section pathology correlated longitudinal study. Journal of Magnetic Resonance Imaging, 2017, 46, 1220-1229.	1.9	2
48	LncRNA GAS5 Inhibits Cellular Proliferation by Targeting P27Kip1. Molecular Cancer Research, 2017, 15, 789-799.	1.5	82
49	Inhibition of BRD4 Suppresses Cell Proliferation and Induces Apoptosis in Renal Cell Carcinoma. Cellular Physiology and Biochemistry, 2017, 41, 1947-1956.	1.1	61
50	LncRNA SPRY4-IT1 sponges miR-101-3p to promote proliferation and metastasis of bladder cancer cells through up-regulating EZH2. Cancer Letters, 2017, 388, 281-291.	3.2	208
51	Co-trained convolutional neural networks for automated detection of prostate cancer in multi-parametric MRI. Medical Image Analysis, 2017, 42, 212-227.	7.0	115
52	Circ <scp>HIPK</scp> 3 sponges miRâ€558 to suppress heparanase expression in bladder cancer cells. EMBO Reports, 2017, 18, 1646-1659.	2.0	474
53	Searching for prostate cancer by fully automated magnetic resonance imaging classification: deep learning versus non-deep learning. Scientific Reports, 2017, 7, 15415.	1.6	131
54	Validation of fast SE-EPI T2 mapping with reference to conventional CPMG T2 mapping, and its application in prostate cancer. , 2017, , .		1

#	Article	IF	CITATIONS
55	Evaluation of different mathematical models and different b-value ranges of diffusion-weighted imaging in peripheral zone prostate cancer detection using b-value up to 4500 s/mm2. PLoS ONE, 2017, 12, e0172127.	1.1	23
56	Prostate Cancer Detection with Multiparametric Magnetic Resonance Imaging. Chinese Medical Journal, 2016, 129, 2451-2459.	0.9	34
57	Rational Use of Computed Tomography for Individual Health Assessment in Asymptomatic Population. Chinese Medical Journal, 2016, 129, 348-356.	0.9	2
58	Androgen ablation elicits PP1-dependence for AR stabilization and transactivation in prostate cancer. Prostate, 2016, 76, 649-661.	1.2	8
59	Ultrasonography-guided percutaneous nephrolithotomy with Chinese one-shot tract dilation technique based on stimulated diuresis: A report of 67 cases. Journal of Huazhong University of Science and Technology [Medical Sciences], 2016, 36, 881-886.	1.0	1
60	BRD4 Regulates EZH2 Transcription through Upregulation of C-MYC and Represents a Novel Therapeutic Target in Bladder Cancer. Molecular Cancer Therapeutics, 2016, 15, 1029-1042.	1.9	96
61	Tuberous sclerosis complex: Imaging characteristics in 11 cases and review of the literature. Journal of Huazhong University of Science and Technology [Medical Sciences], 2016, 36, 601-606.	1.0	3
62	Common and differentially expressed long noncoding RNAs for the characterization of high and low grade bladder cancer. Gene, 2016, 592, 78-85.	1.0	5
63	Flightless I Homolog Represses Prostate Cancer Progression through Targeting Androgen Receptor Signaling. Clinical Cancer Research, 2016, 22, 1531-1544.	3.2	24
64	Correlation of gleason scores with magnetic resonance diffusion tensor imaging in peripheral zone prostate cancer. Journal of Magnetic Resonance Imaging, 2015, 42, 460-467.	1.9	41
65	Long non-coding RNA MEG3 induces renal cell carcinoma cells apoptosis by activating the mitochondrial pathway. Journal of Huazhong University of Science and Technology [Medical Sciences], 2015, 35, 541-545.	1.0	55
66	Comparison of field-of-view (FOV) optimized and constrained undistorted single shot (FOCUS) with conventional DWI for the evaluation of prostate cancer. Clinical Imaging, 2015, 39, 851-855.	0.8	24
67	Feasibility Study of 3-T DWI of the Prostate: Readout-Segmented Versus Single-Shot Echo-Planar Imaging. American Journal of Roentgenology, 2015, 205, 70-76.	1.0	41
68	CAMK2N1 inhibits prostate cancer progression through androgen receptor-dependent signaling. Oncotarget, 2014, 5, 10293-10306.	0.8	52
69	Experience in management of Fournier's gangrene: A report of 24 cases. Journal of Huazhong University of Science and Technology [Medical Sciences], 2012, 32, 719-723.	1.0	8
70	Effect of Smac on TRAIL-induced apoptosis of prostate cancer cell line PC-3 and the molecular mechanism. Journal of Huazhong University of Science and Technology [Medical Sciences], 2012, 32, 233-236.	1.0	1
71	Are histopathological features of prostate cancer lesions associated with identification of extracapsular extension on magnetic resonance imaging?. BJU International, 2010, 106, 1303-1308.	1.3	14
72	Morphological and functional MDCT: problem-solving tool and surrogate biomarker for hepatic disease clinical care and drug discovery in the era of personalized medicine. Hepatic Medicine: Evidence and Research, 2010, 2, 111.	0.9	2

#	Article	IF	CITATIONS
73	Incremental value of magnetic resonance imaging in the advanced management of prostate cancer. World Journal of Radiology, 2009, 1, 3.	0.5	8
74	Effect on proliferation and apoptosis of T24 cell lines via silencing DNMT1 with RNA interference. Frontiers of Medicine in China, 2008, 2, 374-379.	0.1	0
75	Assessment of Biologic Aggressiveness of Prostate Cancer: Correlation of MR Signal Intensity with Gleason Grade after Radical Prostatectomy. Radiology, 2008, 246, 168-176.	3.6	148
76	Prediction of Seminal Vesicle Invasion in Prostate Cancer: Incremental Value of Adding Endorectal MR Imaging to the Kattan Nomogram. Radiology, 2007, 242, 182-188.	3.6	143
77	Incremental Value of Multiplanar Cross-Referencing for Prostate Cancer Staging with Endorectal MRI. American Journal of Roentgenology, 2007, 188, 99-104.	1.0	30
78	Expression of X-linked inhibitor of apoptosis protein and its effect on chemotherapeutic sensitivity of bladder carcinoma. Journal of Huazhong University of Science and Technology [Medical Sciences], 2007, 27, 285-287.	1.0	3
79	Smac/DIABLO promotes mitomycin C-induced apoptosis of bladder cancer T24 cells. Journal of Huazhong University of Science and Technology [Medical Sciences], 2006, 26, 317-318.	1.0	3
80	Prediction of Organ-confined Prostate Cancer: Incremental Value of MR Imaging and MR Spectroscopic Imaging to Staging Nomograms. Radiology, 2006, 238, 597-603.	3.6	237
81	Combined Endorectal and Phased-Array MRI in the Prediction of Pelvic Lymph Node Metastasis in Prostate Cancer. American Journal of Roentgenology, 2006, 186, 743-748.	1.0	83
82	Prostate Cancer: Incremental Value of Endorectal MR Imaging Findings for Prediction of Extracapsular Extension. Radiology, 2004, 232, 133-139.	3.6	205